

# Optical properties of ion exchanged and swift heavy ion beam treated silicate glasses

Ranjana S. Varma<sup>1\*</sup>, D.C. Kothari<sup>1</sup>, A.K. Mallik<sup>2</sup>, A. Bhatnagar<sup>2</sup>, D. Kanjilal<sup>3</sup>, S. Santra<sup>4</sup>, R.G. Thomas<sup>4</sup>, R. Tewari<sup>5</sup>, S. Neogy<sup>5</sup>, G.K. Dey<sup>5</sup>

<sup>1</sup>Department of Physics, and National centre for Nanosciences & Nanotechnology University of Mumbai, Vidyanagari, Santacruz East, Mumbai 400 098, India

<sup>2</sup>SAMEER, IIT Campus, Powai, Post Box No: 8448, Mumbai 400 076, India

<sup>3</sup>Inter-University Accelerator Centre, Aruna Asaf Ali Marg, Post Box 10502, New Delhi, 110067, India

<sup>4</sup>Nuclear Physics Division, Bhabha Atomic Research Centre, Mumbai 400 085, India

<sup>5</sup>Materials Science Division, Bhabha Atomic Research Centre, Mumbai 400 085, India

\*Corresponding author. Tel: (+91) 9821216711; E-mail: ranju16@gmail.com

Received: 14 November 2014, Revised: 27 January 2015 and Accepted: 29 January 2015

## ABSTRACT

Silver ion exchanges on silicate glasses were carried out at different temperatures 320 °C, 400 °C, and 500 °C for 60 min. The exchanged glasses were either annealed at 500 °C for 60 min or swift heavy ion (SHI) irradiated using 120 MeV Ag<sup>9+</sup> ions at a fluence of  $5 \times 10^{12}$  ions/cm<sup>2</sup>. Silver nanoparticles were formed in the samples ion exchanged at 500 °C without any post-exchange treatments. Post-exchange annealing treatment resulted in silver nanoparticle formation for samples ion exchanged at temperature of 320 °C and 400 °C. Whereas post irradiation treatment for ion exchanged sample at 320 °C resulted in Ag<sub>4</sub> nanocluster formation. After post-irradiation, the density of Ag nanoparticles increases for the sample ion exchanged at temperature of 500 °C. RBS was used to obtain silver depth profiles in the ion exchanged samples. Near surface accumulation of Ag atoms is observed in the RBS spectra for the samples prepared at high ion exchange temperature of 500 °C or SHI irradiated samples, in which Ag nanoparticle formation was also observed. UV-vis absorption spectroscopy and Transmission Electron Microscopy (TEM) were used to obtain signatures of nano-particles and to estimate their size. The ion exchanged glasses without nanoparticles were characterized for their possible use in multimode planar waveguides. The post-exchange treated glasses lost their waveguide property, but exhibited nonlinear optical property indicating their potential use for optical switching. Open aperture z-scan measurements for the sample prepared at high ion exchange temperature of 500 °C shows optical limiting behavior, whereas the samples prepared at low ion exchange temperature followed by annealing or irradiation show saturation behavior. Copyright © 2015 VBRI Press.

**Keywords:** Ag nanoparticles; ion exchange; swift heavy ion; z-scan.



**Ranjana Santosh Varma** is working as Women Scientist-A, (DST project) in the Department of Physics, University of Mumbai, India. Her current research interests include synthesis and characterization of nanocomposite materials; ions beam techniques and photocatalysis. She received her PhD degree in Physics in 2009 from University of Mumbai, India.

## Introduction

Glasses containing silver ions and nanoparticles have been used for a long time because of their scientific and technological importance [1-3]. Materials with high values of nonlinear optical parameters such as nonlinear refractive index and absorption coefficient are needed for high-speed

optical switches, effective optical limiters and optical computing because of their ultrafast nonlinear response typically in picoseconds [4-6]. Such materials can be prepared using various methods such as ion exchange, ion implantation, sol gel method followed by annealing and different chemical methods [7-10].

Out of the various techniques, ion exchange is a simple and low cost method to produce metal nanoparticles embedded in the glass matrix [11]. The ion exchange technique for creating optical fiber compatible planar waveguide devices in glass is actively studied and reviewed [12, 13]. Methods, such as laser or thermal annealing are used to modify the particle size and size-distribution of nanoparticles produced in ion-exchanged glasses [14, 15]. Ion-exchange in silicate glasses followed by light ions, heavy ions and electron irradiation is also widely used technique to modify the size and spatial distributions along

with the optical absorption property of metal nanoparticles embedded in glasses [16, 17]. The modification of materials by ion beam is primarily caused by elastic collisions at low (keV) energies whereas electronic excitations and ionizations dominate at high energies (a few tens of MeV and higher). In particular, ion irradiation of silver ion exchanged glasses with light ions promote the aggregation of relatively big clusters, homogeneous in size and distribution, owing to the energy deposited via electronic interaction by the ions of the beam [1, 11].

There are a few reports for production of Ag nanoparticles using ion-exchange in silicate glasses followed by swift heavy ion irradiation [18, 19]. The swift heavy ions (SHIs) irradiation is an excellent tool for the growth, alignment and deformation of embedded nanoparticles in insulating matrices by the high densities of electronic excitations induced by such energetic ions [20, 21]. It has been shown that particles of about the track size are melted in the tracks and re-precipitated with a better size distribution and particles bigger than track radius get elongated along the beam direction [22-24]. Pivin *et al.* [25] has shown that, if sizes of Ag or Au particles are 2 times larger than the molten cylinder of silica then the part of the particle which is outside the cylinder flows more easily in the track and the particle becomes elongated during the freezing stage.

It was shown in our previous work [26] that silver nanoparticles are formed in silver ion exchanged glasses. In this paper a detailed linear and nonlinear optical properties of Ag ion exchange glasses at different ion exchange temperatures followed by irradiation using swift heavy ions are presented. The most interesting and potentially useful advantage in using the ion exchange technique is the possibility of operating subsequent treatments directly in light wave guiding layers, created by the high polarizability of the metal introduced in the glass by the exchange process. The ion exchanged based methods for the synthesis of nanostructured glass composites allow therefore at least in principle to comply with one important technological issue for the application of the composite materials in actual photonic devices, that is, the assembling in light wave guiding components.

## Experimental

### Materials

Commercially available soda lime silicate glasses of sizes 10 x 10 x 1.5 mm were used in the present work. The glass transition temperature of the soda glass is 565 °C and the glass composition in mol. % is as follows: SiO<sub>2</sub> (70.52), Na<sub>2</sub>O (13.84), K<sub>2</sub>O (0.66), CaO (6.98), MgO (5.89), Al<sub>2</sub>O<sub>3</sub> (2.07), and Fe<sub>2</sub>O<sub>3</sub> (0.05). Glass samples for ion exchange were cleaned by acetone and de-ionized water using ultrasonic cleaner.

### Method

The details of sample synthesis have been discussed elsewhere [26]. In short, Ag<sup>+</sup> ion exchange with AgNO<sub>3</sub>:NaNO<sub>3</sub> as 10:90 molar ratios was done at different temperature ranging from 320 °C - 500 °C; annealing and/or irradiation using swift heavy ions (SHI) were

performed after the ion exchange. The sample numbers used in the present work are given in **Table 1**.

**Table 1.** The sample numbers used in the text for silver ion exchanged soda lime silicate glasses (ion exchange at 10:90 molar ratio) at various annealing temperature and/or irradiation using swift heavy ions (SHI).

Sample Number	Exchange Temperature (°C)	Annealing Temperature (°C)	SHI irradiation using 120 MeV Ag <sup>9+</sup> at dose (ion/cm <sup>2</sup> )
1	320	-	-
2	320	500	-
3	320	-	5 x 10 <sup>12</sup>
4	400	-	-
5	400	500	-
6	500	-	-
7	500	500	-
8	500	-	5 x 10 <sup>12</sup>

4 MeV proton beam from Folded Tandem Ion Accelerator (FOTIA) at BARC, Mumbai, was used for Rutherford backscattering (RBS) measurements at backscattering angle of 160°. The RBS data was fitted with Rutherford Universal Manipulation Program (RUMP) code [27]. The planar waveguide formed after ion exchange was tested using an automated prism coupled method. He-Ne laser with a wavelength  $\lambda = 632.8$  nm and a polarization appropriate for TE mode excitation was used as a radiation source. From the set of refractive indices, determined from the measured angles, the refractive index profiles of the waveguides were reconstructed by inverse WKB procedures. This particular technique does not make any assumptions about the index profile shape apart from it being monotonically decreasing.

The size of Ag nanoparticle was obtained from the width of the SPR peak observed in UV-vis absorption spectra and also from the Transmission Electron Microscopy (TEM) images obtained (for some samples) from JEOL 2000 FX Transmission Electron Microscope (TEM), operated at an accelerating voltage of 160 kV. The details of sample preparation for the TEM measurement of the ion exchanged planar glass are reported in our previous work [26]; in brief, the glass surface containing silver nanoparticle was scratched with a diamond glass cutter and fine powder obtained was ultrasonically agitated in methanol. A drop of methanol containing glass powder after agitation was placed on a carbon coated copper grids for the TEM imaging. Cross-sectional TEM image was obtained for the SHI irradiated sample. For this, first the slices of the samples (0.5 mm) were cut and two slices were glued with epoxy onto copper grid having 1 mm hole in the centre side by side in such a way that the interface is parallel to the electron beam during the TEM imaging. This assembly was then disk polished and ion milled in liquid nitrogen to avoid damage due to heating during ion milling prior to the TEM imaging. Optical nonlinearity in the prepared samples was determined using the open aperture z scan method. The measurements of the nonlinear optical transmission at 532 nm were made with an Nd:YAG laser (pulse width = 5 ns).

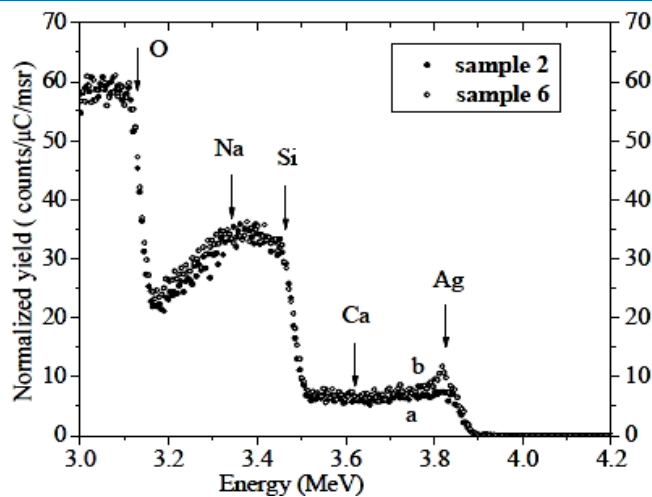


**Fig. 1.** RBS spectra of Ag ion exchanged glasses at two different temperatures (a) Sample-1: 320 °C (b) Sample-6: 500 °C in soda lime silicate glasses.

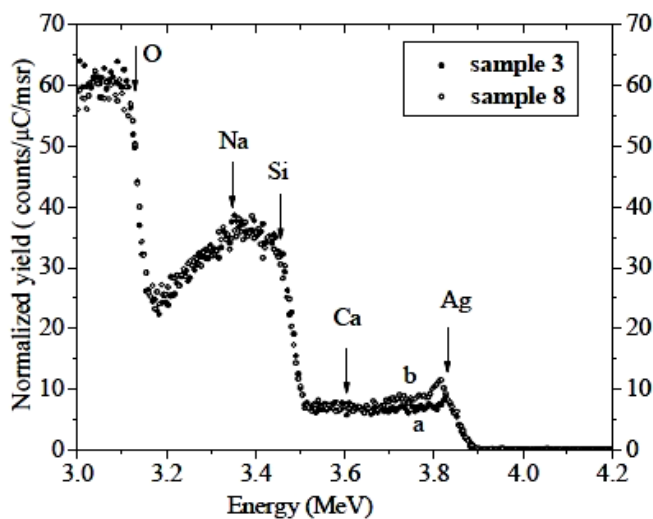


**Fig. 2.** RBS spectra of Ag ion exchanged glasses at two different temperatures (a) Sample-3: 320 °C (b) Sample-8: 500 °C followed by SHI irradiation using 120 MeV  $\text{Ag}^{9+}$  ion at dose of  $5 \times 10^{12}$  ion/cm<sup>2</sup> in soda lime silicate glasses.

## Results and discussion

The RBS spectra of Sample-1 and Sample-6 for the silver ion exchanged glasses at two different ion exchange temperatures of 320 °C and 500 °C are shown in **Fig. 1**. In **Fig. 2**, the RBS spectra of Sample-3 and Sample-8 for ion exchanged samples followed by SHI irradiation are shown. The backscattering data was analyzed with the help of RUMP software [27]. In **Fig. 1** and **Fig. 2** signals corresponding to the scatterings from sodium, silicon, calcium, oxygen, and silver atoms on the surface of the samples are indicated by arrows. In **Fig. 1 (b)** for Sample-6 ion exchanged at temperature of 500 °C, a peak appears in the silver signal, indicating an accumulation of silver element at a depth of about 250 nm (obtained from RUMP fitting [27]). Similar accumulation of silver is reported [28] for ion exchanged samples followed by annealing. The surface accumulation of silver atoms can be understood as follows: during the silver ion exchange large  $\text{Ag}^+$  ions enter the glass structure and replace the smaller  $\text{Na}^+$  ions. Due to

the size difference between the  $\text{Ag}^+$  and  $\text{Na}^+$  ions, a tensile stress is introduced in the surface region [26, 28]. At high temperature ion exchange,  $\text{Ag}^+$  ions diffuse in the surface region [26] and reduce the tensile stress. Thus more Ag atoms are available in the surface region, which eventually become Ag nanoparticle (here nanoparticle means clusters of more than 20 atoms and less than 200 hundred atoms) as observed in absorption spectra shown later.

It can be inferred that for Sample-6, the growth of Ag nanoparticles might be taking place within a depth of ~ 250 nm below the glass surface after ion exchange at 500 °C; though, silver atoms are present up to 10 μm from the surface of the glass, as revealed by RBS investigations for as exchanged samples. Sample-3 and Sample-8, corresponding to the ion exchange at 320 °C and 500 °C respectively, after irradiation with 120 MeV  $\text{Ag}^{9+}$  ions at a dose of  $5 \times 10^{12}$  ion/cm<sup>2</sup>, show similar accumulation in the near surface region. In fact, for the sample ion exchanged at 320 °C for which no accumulation was observed, after irradiation, the accumulation of silver element at a depth of about 100 nm is observed (obtained from RUMP fitting [27]). And for the sample ion exchanged at 500 °C, accumulation of silver element at a depth of about 350 nm is observed (obtained from RUMP fitting [27]); that is after irradiation the depth of silver accumulation has increased by 100 nm.

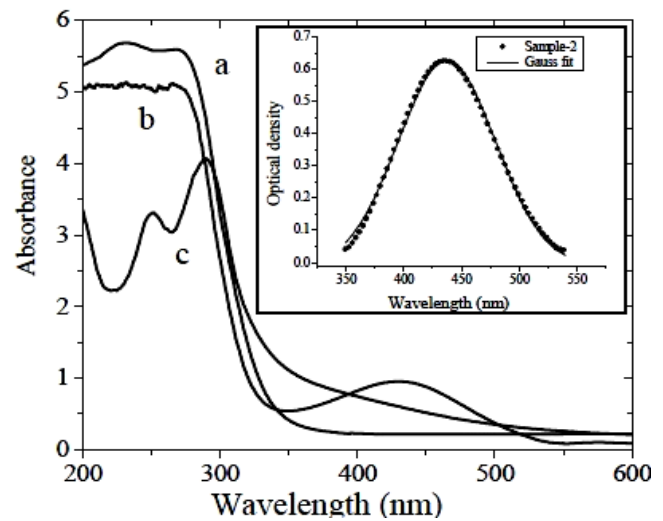


**Fig. 3.** Absorption spectra of the silver ion exchanged glass sample with molar ratio 10:90 (a) Sample-1: ion exchanged at 320 °C for 60 min; (b) Sample-2: ion exchanged at 320 °C for 60 min and annealed at 500 °C; (c) Sample-3: ion exchanged at 320 °C for 60 min followed by SHI irradiation (inset in the Fig. 3 is the Gaussian fit to the SPR peak).

The absorption spectra for Sample-1, Sample-2 and Sample-3 are shown in **Fig 3**. Inset in **Fig. 3** shows the Gaussian fit to the SPR peak of Ag nanoparticles. In **Fig. 3** for curve 'a' and curve 'b', the observed flat band in the UV region of the absorption spectrum is due to the presence of  $\text{Ag}^+$  ions and their complexes present in the soda glass [26]. After annealing  $\text{Ag}^+$  ions present in the soda glass are converted to Ag nanoparticles, as indicated by a peak at 425 nm in the absorption spectrum [26] (curve 'b'). The curve 'c' shows the absorption spectrum for sample ion exchanged at 320 °C followed by irradiation using 120 MeV  $\text{Ag}^{9+}$  at a dose of  $5 \times 10^{12}$  ion/cm<sup>2</sup>. The

absorption spectra show peaks at wavelengths of about 251 nm and 290 nm and SPR peak due to Ag nanoparticles is not observed. The absorption peaks at 251 nm and 290 nm are assigned to the presence of  $Ag_4$  cluster [29-31]. The inset in Fig. 3 shows the data for Sample-2, after baseline correction. The Fig. 3 also shows a Gaussian fit to the experimental data. The average diameter of the Ag nanoparticle is 2.85 nm, calculated using the Mie's theory [32].

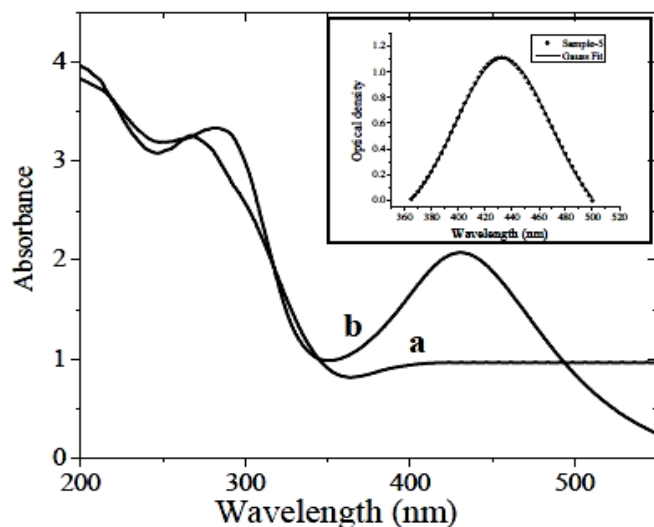


**Fig. 4.** Absorption spectra of the silver ion exchange glass sample with molar ratio 10:90 (a) Sample-4: ion exchanged at 400 °C for 60 min; (b) Sample-5: ion exchanged at 500 °C for 60 min and annealed at 400 °C. (inset in the Fig. 4 is the Gaussian fit to the SPR peak).

**Fig. 4** shows the absorption spectra for Sample-4 and Sample-5 corresponding to the ion exchange at 400 °C and ion exchange followed by annealing at 500 °C in air for 60 min respectively. A behavior similar to that observed for the sample ion exchanged at 320 °C is observed, band in the UV region of ion exchange glass corresponds to the presence of  $Ag^+$  and their complexes and a broad band in the region of 425 nm absorption is due to the presence of Ag nanoparticles. During annealing these  $Ag^+$  ions are converted to Ag atoms and Ag nanoparticles as indicated by a band at 300 nm and a peak in the region of 425 nm in the absorption spectra (curve 'b'). The diameter of the Ag nanoparticles was obtained as 3.28 nm from the Mie's theory [32] for Sample 5.

**Fig. 5 (a)** and **Fig. 5 (b)** show the absorption spectra of Sample-6, Sample-7 and Sample-8 for ion exchanged at 500 °C, ion exchange followed by annealing at 500 °C in air for 1 hr and to the ion exchange at 500 °C followed by 120 MeV  $Ag^{9+}$  irradiation at a dose of  $5 \times 10^{12}$  ion/cm<sup>2</sup>, respectively. The curve 'a' shows a broad band in the region of 200-250 nm and two peaks at 305 nm and 425 nm. The broad band in the curve 'a' corresponds to the presence of  $Ag^+$  and their complexes [26] and the peaks at 305 nm and 425 nm of ion exchanged glass at 500 °C corresponds to the presence of  $Ag^0$  atoms and Ag nanoparticles respectively. Annealing at 500 °C of ion exchanged glass at 500 °C, curve 'b' shows a clear peak at 305 nm due to  $Ag^0$  atoms and 425 nm peaks due to presence of Ag nanoparticle. The increase in the intensity

of 425 nm absorption peak is due to the increase in number density of Ag nanoparticles after annealing. The curve 'c' shows peaks at 315 nm and 425 nm corresponding to the presence of  $Ag^0$  atom [31] and Ag nanoparticles respectively [26].

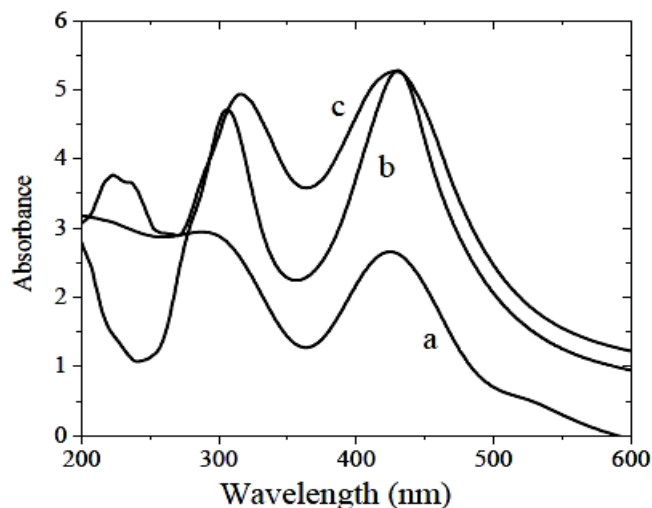


**Fig. 5.** Absorption spectra of the silver ion exchanged glass sample with molar ratio 10:90 (a) Sample-6: ion exchanged at 500 °C for 60 min; (b) Sample-7: ion exchanged at 500 °C for 60 min and annealed at 500 °C; (c) Sample-8: ion exchanged at 500 °C for 60 min followed by SHI irradiation.

**Fig. 6** shows the Gaussian fit to the SPR peak of Ag nanoparticles after baseline correction. The diameters of the Ag nanoparticle from Mie's theory [32] are 3.72 nm, 5.47 nm and 3.98 nm for Sample-6, Sample-7 and Sample-8 corresponding to the sample ion exchanged at 500 °C, the sample ion exchanged at 500 °C followed by annealing at 500 °C and sample ion exchanged at 500 °C followed by SHI irradiation respectively.

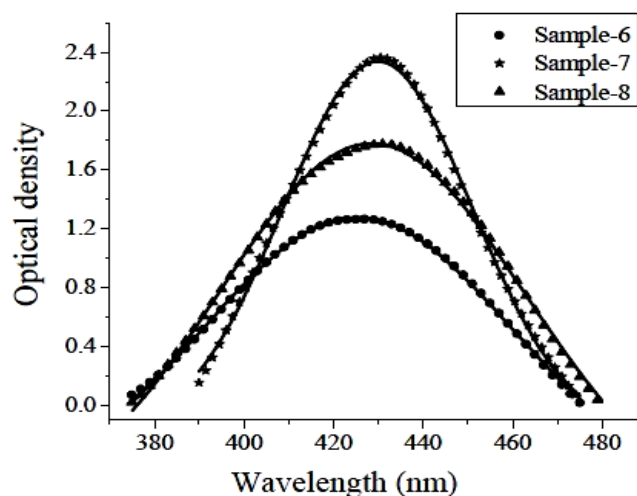


**Fig. 6.** SPR peak of the absorption spectra for the silver ion exchanged glass sample with molar ratio 10:90 (a) Sample-6: ion exchanged at 500 °C for 60 min; (b) Sample-7: ion exchanged at 500 °C for 60 min and annealed at 500 °C; (c) Sample-8: ion exchanged at 500 °C for 60 min followed by SHI irradiation.

In **Fig. 7**, the curves 'a' and 'b' represent refractive index profiles constructed from the modes obtained by inverse WKB method for the sample ion exchanged at

temperature of 320 °C and 400 °C for 60 min respectively. For Sample 1 and Sample-4 corresponding to the ion exchange at 320 °C and 400 °C for 60 min, the numbers of modes obtained in prism coupling are 9 and 17 respectively. But, the samples ion exchanged at high temperature of 500 °C or annealed samples or irradiated samples do not show any modes. The refractive index profiles for the samples ion exchanged at temperatures of 320 °C and 400 °C extend up to 9.98  $\mu\text{m}$  and 10.8  $\mu\text{m}$  respectively, which correlate with the Ag atom depth profiles obtained from the RBS spectra. The difference in refractive indices ( $\Delta n$ ) of samples before and after ion exchange fulfills the condition  $\Delta n \leq 0.075$  for the waveguide applications [2].

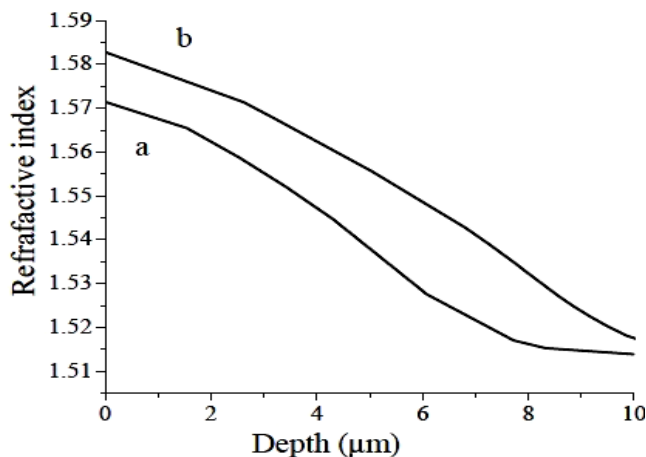


**Fig. 7.** Refractive index profile for sample ion exchange at (a) Sample-1: 320 °C (b) Sample-4: 400 °C; for 60 min.

**Fig. 8** shows the Transmission electron microscopy (TEM) image and size distribution of nanoparticles obtained from the image analysis, for Sample-2 corresponding to the ion exchange at 320 °C followed by annealing at 500 °C. The average diameter of nanoparticles obtained from the histogram in **Fig. 8 (b)** is 2.81 nm, in agreement of the diameter obtained from SPR peak in the absorption spectra (2.85 nm). The average diameter for Sample-6 corresponding to the ion exchange at 500 °C is 3.72 nm [26]. **Fig. 9** shows the cross sectional TEM image and size distribution for Sample-8 corresponding to the ion exchange at 500 °C followed by SHI irradiation at a dose of  $5 \times 10^{12}$  ion/cm<sup>2</sup>. The average diameter of Ag nanoparticles obtained from TEM is 3.90 nm for Samples-8, which correlates well with the diameter obtained from the SPR peak in the absorption spectra as 3.98 nm. It is reported that, for spherical nanoparticle of sizes about the track radius, the particles are melted in the tracks and re-precipitated with a better size distribution and for bigger particles than track radius elongation along the beam direction was observed [22-24]. In our case the particles sizes were nearly the same as the track diameter and we have observed growth of nanoparticles with better size distribution after SHI irradiation and no deformation of particles were observed as expected. Whereas, the density and depth distribution of the nanoparticles were increases after SHI irradiation as observed in absorption spectra and RBS spectroscopy.

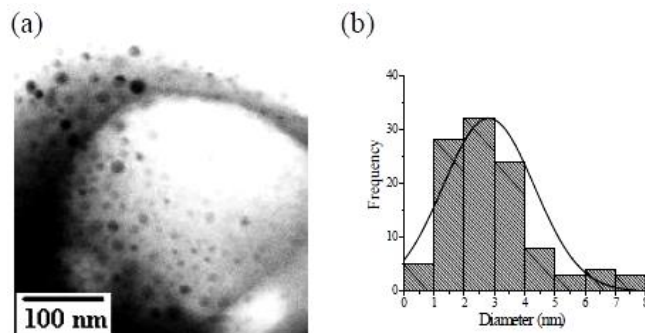


**Fig. 8.** (a) TEM image showing the presence of silver nanoparticles in Sample-2: sample ion exchanged with molar ratio of 10:90 at 320 °C for 60 min followed by annealed at 500 °C for 1 hr and (b) frequency distribution of the diameters of nanoparticles from the TEM image.

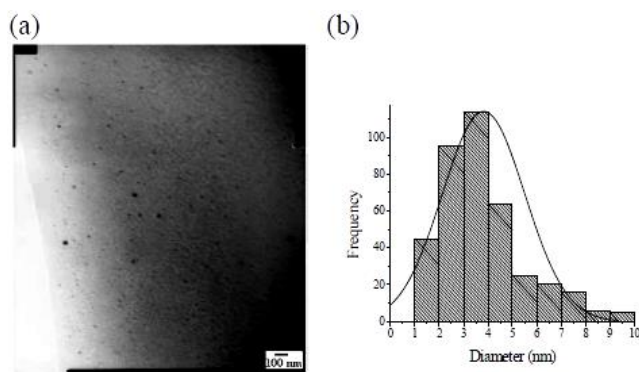


**Fig. 9.** (a) Cross sectional TEM image for Sample-8: soda glass ion exchanged with molar ratio 10:90 at 500 °C for 60 min followed by SHI irradiation and (b) frequency distribution of the diameters of nanoparticles from the TEM image.

**Fig. 10 (a)-(d)** show the results of open-aperture z-scan for Sample-1, Sample-2, Sample-6 and Sample-8 respectively. Nonlinearity is not observed for Sample-1 corresponding to the ion exchange at 320 °C without annealing as shown in **Fig. 10 (a)**, in which Ag nanoparticles were not present. For Sample-2 at laser energy of 100  $\mu\text{J}$  the effect of absorption saturation is very small. However at laser energy of about 200  $\mu\text{J}$ , clear absorption saturation is observed as shown in **Fig. 10 (b)**. For the samples ion exchanged at 500 °C (**Fig. 10 (c)**) and for sample ion exchanged at 500 °C for 60 min followed by SHI irradiation (**Fig. 10 (d)**), the value of ( $\beta$ ) is positive (decrease in transmission). Virgin soda lime glass without any treatment did not show any nonlinearity (not shown here) and hence we can conclude that the origin of the optical nonlinearity in all the investigated samples is due to the presence of metal nanoparticles. In short, for samples ion exchanged at 320 °C followed by annealing saturation of absorption occurs, while for samples ion exchanged at 500 °C, optical limiting behavior is observed.

When the metal nanoparticles are embedded in a dielectric matrix, the experimentally measured effective optical susceptibility of the composite material  $\chi^{(3)}$  is related to  $\chi_m^{(3)}$  [33].

$$\chi^{(3)} = p \cdot f^2 \cdot |f|^2 \cdot \chi_m^{(3)} \quad (1)$$

Where,  $p$  is the volume fraction of nanoparticles, and  $f = 3\epsilon_0 / (\epsilon + 2\epsilon_0)$  is the local field effect (with  $\epsilon_0$  and  $\epsilon$  being the dielectric constants of the matrix and metal, respectively). Near the SPR,  $\epsilon + 2\epsilon_0 = 0$ ,  $f$  becomes resonant and  $\chi^{(3)}$  is thus enhanced by local field effects.

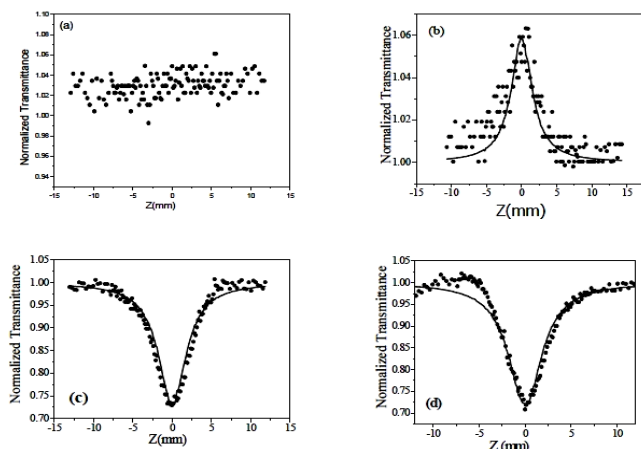


**Fig. 10.** Open aperture z-scan plots for silver ion exchanged glass sample with molar ratio 10:90 (a) Sample-1: ion exchanged at 320 °C for 60 min (b) Sample-2: ion exchanged at 320 °C for 60 min and annealed at 500 °C; (c) sample 6: ion exchanged at 500 °C for 60 min; (d) Sample-8: ion exchanged at 500 °C for 60 min followed by SHI irradiation. (Line through solid circle representing the experimental data is saturable absorption or two photon absorption fit to the experimental data).

From Eq. (1) it is clear that  $\chi^{(3)}$  depends both on the nanoparticle diameter (through  $\chi_m^{(3)}$ ) and on the metal volume fraction, ( $p$ ).

At high ion exchange temperature (500 °C), the nanoparticles density is higher than that in the sample ion exchanged at a lower temperature of 320 °C followed by annealing (Figs. 3 and Fig. 5).

From the observed increase in the density of nanoparticles (seen in absorption spectra), for the sample ion exchanged at high exchange temperature we can say that the difference in the observed behaviors in z-scan results (i.e. optical limiting or saturable absorption) for the present samples are mainly due to the changes in density of the nanoparticles (i.e. the volume fraction  $p$  of nanoparticles in Eqn. 1).

The experimental data is found to fit well with a two photon absorption process [34] given by Eq. (2) or with a saturable absorption process given by Eq. (3),

$$T = \left( (1-R)^2 \exp(-\alpha_0 L) / \sqrt{\pi} q_0 \right) \int_{-\infty}^{+\infty} \ln[1 + q_0 \exp(-t^2)] dt \quad (2)$$

where,  $q_0 = \beta(1-R)I_0 L_{eff}$  and  $L_{eff} = (1 - e^{-\alpha_0 L}) / \alpha_0$

$$\frac{dI}{dz} = - \left[ \frac{\alpha_0}{1 + I_0/I_s} \right] I_0 \quad (3)$$

Here  $T$  is the net transmission of the samples,  $L$  and  $R$  are the sample length and surface reflectivity respectively,

$\alpha_0$  is the linear absorption coefficient,  $I_0$  is the on-axis peak intensity, and  $\beta$  is the two-photon absorption coefficient,  $z$  is the propagation distance and  $I_s$  is the saturation intensity. The value of two photon absorption coefficient  $\beta$  and the value of the saturation intensity  $I_s$  calculated from numerical fits to the experimental data are given in Table 2. The summaries of data obtained from various measurements are also given in Table 2.

In summary, we can say that the, metal ions are first introduced in a superficial region of the glass (of typical thickness up to several micrometers) by means of an ion exchange procedure. In this way, depending on the metal, an optical waveguide may be formed, in which high metal concentration values can be reached without precipitation. Suitable annealing treatments then promote the aggregation of dimers, multimers and eventually very small nanoparticles, throughout the whole exchanged region.

And, further cluster growth may be then obtained by means of SHI irradiation, by which it is possible to form spherical nanoparticles with better size distribution. Thus, the obtained, ion exchanged glasses with silver nanoparticles can be used for nonlinear application as confirmed from the z-scan measurements.

**Table 2.** The summary of data obtained from various measurements.

Sample Number	Diameter of Ag nanoparticle (nm)	RBS (Ag accumulation depth) nm	Number of modes observed in prism coupling	z-scan results			
				E (mJ)	b (m/W)	$I_s$ (W/m <sup>2</sup> )	Sign of nonlinear absorption coefficient
1	No Ag nanoparticles	-	No	9	-	-	-
2	2.85	2.81	-	No	200	-	$5 \times 10^{14}$ -ve
3	No Ag nanoparticles, Ag <sub>4</sub> clusters	-	-	No	-	-	-
4	No Ag nanoparticles	-	-	17	-	-	-
5	3.28	-	-	No	-	-	-
6	3.72	3.75 [24]	~250 nm	No	100	$9.5 \times 10^9$	+ve
7	5.47	-	~100 nm	No	-	-	-
8	3.98	3.90	~350 nm	No	100	$11.3 \times 10^9$	+ve

## Conclusion

Silver nanoparticles were formed in the samples ion exchanged at 500 °C without any post-exchange treatments. Post-exchange annealing treatment resulted in silver nanoparticle formation for samples ion exchanged at temperature of 320 °C and 400 °C. Whereas post irradiation treatment for ion exchanged sample at 320 °C resulted in Ag<sub>4</sub> nanocluster formation. After post-irradiation, the density of Ag nanoparticles increases for the sample ion exchanged at temperature of 500 °C. Near surface accumulation of Ag atoms is observed in the RBS spectra for the samples prepared at high ion exchange temperature of 500 °C or SHI irradiated samples, in which Ag nanoparticle formation was also observed. The size of nanoparticles obtained from the absorption spectra and TEM measurements are in agreement. The post-exchange treated glasses lost their waveguide property, but exhibited nonlinear optical property indicating their potential use for optical switching. Open aperture z-scan measurements for the sample prepared at high ion exchange temperature of 500 °C shows optical limiting behavior, whereas the samples prepared at low ion exchange temperature

followed by annealing or irradiation show saturation behavior. The change in optical nonlinearity observed in the prepared sample is expected to be due to the change in density of the nanoparticles present in the samples.

### Acknowledgements

This work was supported by the Inter-University Accelerator Centre, New Delhi. The authors are indebted to CSS Sandeep and R. Philip (Nonlinear optics lab of Raman Research Institute, Bangalore, India) for doing the Nonlinear measurements. The authors are indebted to Pelletron group at IUAC, New Delhi for assistance during the Ag-ion irradiations and NPD group from BARC, Mumbai for assistance during the RBS experiments at BARC.

### Reference

- Marchi, G.D.; Gonella, F.; Mazzoldi, P.; Battaglin, G.; Knystautas, E.J.; Meneghini, C.; *J of Non-Crystalline Solids*, **1996**, 196, 79.  
DOI: [10.1016/0022-3093\(95\)00551-X](https://doi.org/10.1016/0022-3093(95)00551-X)
- Chen, S.; Akai, T.; Kadono, K.; Yazawa, T.; *Appl. Phys. Lett.*, **2001**, 79 (22), 3687.  
DOI: [10.1063/1.1418257](https://doi.org/10.1063/1.1418257)
- Obraztsov, P.A.; Nashchekin, A.V.; Nikonorov, N.V.; Sidorov, A.I.; Panfilova, A.V.; Brankor, P.N.; *Physics of the solid state*, **2013**, 55 (6), 1272.  
DOI: [10.1134/S106383413060267](https://doi.org/10.1134/S106383413060267)
- Kapoustine, V.V.; Sannikov, D.G.; Kazakevitch, A.V.; *Optics Communications*, **2002**, 205, 87.  
DOI: [10.1016/S0030-4018\(02\)01254-3](https://doi.org/10.1016/S0030-4018(02)01254-3)
- Sun, Y.P.; Riggs, J.E.; Henbest, K.B.; Martin, R.B.; *J. Nonlinear Opt. Phys. Mater.*, **2000**, 9(4), 481.  
DOI: [10.1142/S0218863500000315](https://doi.org/10.1142/S0218863500000315)
- Sato, R.; Ohnuma, M.; Oyoshi, K.; Takeda, Y.; *Phys. Rev. B.*, **2014**, 90, 125417  
DOI: [10.1103/PhysRevB.90.125417](https://doi.org/10.1103/PhysRevB.90.125417)
- Quaranta, A.; Cattaruzza, E.; Gonella, F.; Rahman, A.; Mariotto, G.; *J.of Non-Cryst. Solids*, **2014**, 401, 219.  
DOI: [10.1016/j.jnoncrystalsol.2013.12.041](https://doi.org/10.1016/j.jnoncrystalsol.2013.12.041)
- Dubiel, M.; Hofmeister, H.; Tan, G.L.; Schicke K.D.; Wendler, E.; *Eur. Phys. J. D.*, **2003**, 24, 361.  
DOI: [10.1140/epjd/e2003-00178-5](https://doi.org/10.1140/epjd/e2003-00178-5)
- Li, W.; Seal, S.; Megan, E.; Ramsdell, J.; Scammon, K.; *J. of Appl. Phys.*, **2003**, 93 (12), 9553.  
DOI: [10.1063/1.1571215](https://doi.org/10.1063/1.1571215)
- Hedayati, M. K.; Faupel, F.; Elbahri, M.; *Materials*, **2014**, 7 (2), 1221.  
DOI: [10.3390/ma7021221](https://doi.org/10.3390/ma7021221)
- Mazzoldi, P.; Carturan, S.; Quaranta, A.; Sad, C.; Sglavo, V.M.; *Rivista Del Nuovo Cimento*, **2013**, 36 (9), 397  
DOI: [10.1393/ncr/i2013-10092-1](https://doi.org/10.1393/ncr/i2013-10092-1)
- Bogle, K.A.; Dhole, S.D.; Bhoraskar, V. N.; *Nanotechnology* **2006**, 17, 3204  
DOI: [10.1088/0957-4484/17/13/021](https://doi.org/10.1088/0957-4484/17/13/021)
- Lal, S.; Link, S.; Halas, N.J.; *Nature photonics*, **2007**, 1, 641.  
DOI: [10.1038/nphoton.2007.223](https://doi.org/10.1038/nphoton.2007.223)
- G. Stewar, C. A. Millar, P. J. R. Laybourn, C. D. W. Wilkinson and R. M. Delarue; *IEEE J. of Quantum Electronics*, **1977**, 13 (4), 192.  
DOI: [10.1109/JQE.1977.1069321](https://doi.org/10.1109/JQE.1977.1069321)
- Jose, G.; Sorbello, G.; Taccheo, S.; Della Valle, G.; Cianci, E.; Foglietti, V.; Laporta, P.; *Opt. Mater.*, **2003**, 23 (3-4), 559.  
DOI: [10.1016/S0925-3467\(03\)00021-1](https://doi.org/10.1016/S0925-3467(03)00021-1)
- Gonella, F.; Mattei, G.; Mazoldi, P.; Cattaruzza, E.; Arnold, G.W.; Battaglin, G.; Calvelli, P.; Polloni, R.; Bertencello, R.; Haglund, R.F.; *Appl. Phys. Lett.*, **1996**, 69, 3101.  
DOI: [10.1063/1.117318](https://doi.org/10.1063/1.117318)
- Peters, D.P.; Strohhofer, C.; Brongersma, M.L.; J. van der Elsken and A. Polman; *Nucl. Instr. and Meth. in Phys. Res. B*, **2000**, 168, 237.  
DOI: [10.1016/S0168-583X\(99\)00891-5](https://doi.org/10.1016/S0168-583X(99)00891-5)
- Mahnke, H.E.; Schattat, B.; Schubert-Bischoff, P.; Novakovic, N.; *Nucl. Instr. and Meth. in Phys. Res. B*, **2006**, 245, 222.  
DOI: [10.1016/j.nimb.2005.11.105](https://doi.org/10.1016/j.nimb.2005.11.105)
- Mahnke, H. E.; Zizak, I.; Schubert- P. Bischoff and V. Koteski; *Materials Science and Engineering B*, **2008**, 149, 200.  
DOI: [10.1016/j.mseb.2007.11.036](https://doi.org/10.1016/j.mseb.2007.11.036)
- Singh, F.; Mohapatra, S.; Stoquert, J.P.; Avasthi, D.K.; Pivin, J.C.; *Nucl. Instr. and Meth. in Phys. Res. B.*, **2009**, 267, 936.  
DOI: [10.1016/j.nimb.2009.02.026](https://doi.org/10.1016/j.nimb.2009.02.026)
- Itoh, N.; Duffy, D.M.; Khakshouri, S.; Stoneham, A.M.; *J. Phys.: Condens. Matter*, **2009**, 21, 474205.  
DOI: [10.1088/0953-8984/21/47/474205](https://doi.org/10.1088/0953-8984/21/47/474205)
- Yang, Y.; Zhang, C.; Song, Y.; Gou, J.; Zhang, L.; Meng, Y.; Zhang, H.; Ma, Y.; *Nucl. Instr. and Meth. in Phys. Res. B.*, **2013**, 308, 24.  
DOI: [10.1016/j.nimb.2013.05.004](https://doi.org/10.1016/j.nimb.2013.05.004)
- Dufour, C.; Khomenkov, V.; Rizza, G.; Toulemonde, M.; *J. Phys. D: Appl. Phys.*, **2012**, 45, 065302.  
DOI: [10.1088/0022-3727/45/6/065302](https://doi.org/10.1088/0022-3727/45/6/065302)
- Singh, F.; Pivin, J.C.; Dimova-Malinovska, D.; Stoquert, J.P.; *J. Phys. D: Appl. Phys.*, **2011**, 44, 325101.  
DOI: [10.1088/0022-3727/44/32/325101](https://doi.org/10.1088/0022-3727/44/32/325101)
- Pivin, J.C.; Singh, F.; Mishra, Y.; Avasthi, D.K.; Stoquert, J.P.; *Surf. & Coat. Tech.*, **2009**, 203, 2432.  
DOI: [10.1016/j.surfcoat.2009.02.033](https://doi.org/10.1016/j.surfcoat.2009.02.033)
- Varma, R.S.; Kothari, D.C.; Tewari, R.; *J.of Non-Cryst. Solids*, **2009**, 355 (22-23), 1246.  
DOI: [10.1016/j.jnoncrystalsol.2009.05.001](https://doi.org/10.1016/j.jnoncrystalsol.2009.05.001)
- Doolittle, L. R.; *Nucl. Instr. and Meth. in Phys. Res. B.*, **1985**, 9, 344.  
DOI: [10.1016/0168-583X\(85\)90762-1](https://doi.org/10.1016/0168-583X(85)90762-1)
- Gangopadhyay, P.; Magudapathy, P.; Kesavamoorthy, R.; Panigrahi, B.K.; Nair, K.G.M.; Satyam, P.V.; *Chemical Physics Letters*, **2004**, 388, 416.  
DOI: [10.1016/j.cplett.2004.03.055](https://doi.org/10.1016/j.cplett.2004.03.055)
- Fedrigo, S.; Harbich, W.; Buttet, J.; *J. Chem. Phys.*, **1993**, 99, 5712.  
DOI: [10.1063/1.465920](https://doi.org/10.1063/1.465920)
- Koutecky, V.B.; Pittner, J.; Boiron, M.; Fantucci, P.; *J. of Chem. Phys.*, **1999**, 110 (8), 3876.  
DOI: [10.1063/1.478242](https://doi.org/10.1063/1.478242)
- Harb, M.; Rabilloud, F.; Simon, D.; Rydlo, A.; Lecoulter, S.; Conus, F.; Rodrigues, V.; Felix, C.; *J of Chem. Phys.*, **2008**, 129, 194108.  
DOI: [10.1063/1.3013557](https://doi.org/10.1063/1.3013557)
- Varma, R.S.; Kothari, D.C.; Choudhari, R.J.; Kumar, R.; Tewari R.; Dey, G.K; *Surf. Coat. & Tech.*, **2009**, 203, 2468.  
DOI: [10.1016/j.surfcoat.2009.02.080](https://doi.org/10.1016/j.surfcoat.2009.02.080)
- Palpant, B.; Third-order nonlinear optical response of metal nanoparticles, In: Papadopoulos, M.G; Sadlej, A.J.; Leszczynski, J.; (eds.), Non-Linear Optical Properties of Matter, Springer **2006**.  
DOI: [10.1007/1-4020-4850-5\\_12](https://doi.org/10.1007/1-4020-4850-5_12)
- Sutherland, R.L.; 'Handbook of Nonlinear Optics', second ed. Dekker, New York, **2003**  
DOI: [10.1007/9780824742430](https://doi.org/10.1007/9780824742430)

### Advanced Materials Letters

Copyright © VBRI Press AB, Sweden  
[www.vbripress.com](http://www.vbripress.com)

Publish your article in this journal

Advanced Materials Letters is an official international journal of International Association of Advanced Materials (IAAM, [www.iaamonline.org](http://www.iaamonline.org)) published monthly by VBRI Press AB, Sweden. The journal is intended to provide top-quality peer-review articles in the fascinating field of materials science and technology particularly in the area of structure, synthesis and processing, characterisation, advanced-state properties, and application of materials. All published articles are indexed in various databases and are available download for free. The manuscript management system is completely electronic and has fast and fair peer-review process. The journal includes review article, research article, notes, letter to editor and short communications.

